Reports

Lung Water Quantitation by Nuclear Magnetic Resonance Imaging

Abstract. *Nuclear magnetic resonance imaging was used to determine quantitatively the water distribution of saline-filled and normal rat lungs in both isolated lung and in situ preparations. Regional lung edema was easily detected. Studies of an isolated lung fragment indicate an accuracy of better than 1 percent and images of H_2O/D_2O phantoms indicate an average error of 2.7 percent.*

Nuclear magnetic resonance (NMR) imaging has been increasingly used in recent years to determine the spatial distribution of water in intact animals (*1*) and humans (*2*). Since the formation of edema is a fundamental element in the response of lung to injuries of many kinds, the measurement of lung water is of major physiological and clinical interest.

Although a variety of techniques for obtaining images by NMR measurements have been developed, application of these techniques to pulmonary studies has been limited. The only data reported in the literature are those of Lauterbur (*3*) and Frank (*4*), who studied the relation between the spin-lattice relaxation time T_1 and the dry-to-wet lung weight ratio (*D/W*) in vitro. They observed a linear relation between the spin-lattice relaxation rate $1/T_1$ and *D/W* and concluded that it may be feasible to use NMR imaging to detect pulmonary edema, even in the early stages (*3*). However, published NMR imaging data on lungs have been qualitative and visual; to our knowledge, no quantitative data derived from NMR images have been reported.

For the quantitation of lung water, NMR imaging has several advantages over gravimetric, double-indicator dilution, soluble gas, and other methods (*5*). The NMR measurements are noninvasive and nondestructive, do not require the use of indicator tracers, are independent of the distribution of ventilation and perfusion, and provide a high degree of spatial resolution.

We report here the results of experiments on phantoms as well as on excised and in situ rat lungs. These experiments establish the quantitative nature of NMR imaging and demonstrate the feasibility and validity of NMR measurements of lung water content and distribution in both edematous and nonedematous lungs.

In a conventional nonimaging NMR experiment, a specimen placed in a large static magnetic field is subjected to a small radio-frequency (RF) field at the natural precession (Larmor) frequency of the nucleus to be studied (*6*). Only nuclei of the atomic species whose Larmor frequency corresponds to the RF frequency will be excited. However, nuclei of the same species in different locations in the same field will not be resolvable. In contrast, in an NMR imaging experiment, spatial resolution is achieved by superimposing a field gradient (a spatially varying field) on the static magnetic field. Nuclei at different locations will then be resolvable since their Larmor frequencies are different by virtue of the positional variation of the magnetic field.

The data reported here were taken at 40 MHz in a 12-inch Varian electromagnet with a 3¼-inch gap (originally purchased for solid-state physics studies). Since the region over which the magnetic field was homogeneous was considerably smaller than the intact rats studied, we used a line-scan technique similar to one developed at the University of California, San Francisco (*7*). With this technique, images are constructed one line at a time. The water distribution (proton density) in one line is obtained by the

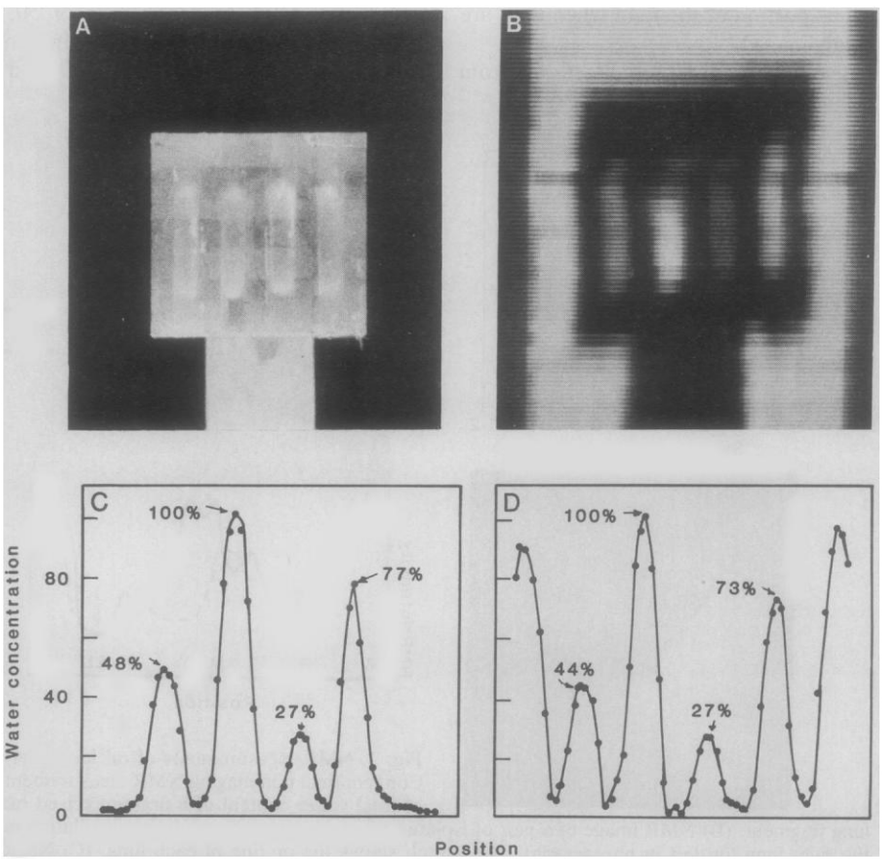

Fig. 1. NMR images of water distribution in a simulated chest cavity. (A) Frontal (en face) view of Plexiglas phantom with four chambers containing mixtures of H_2O and D_2O. The H_2O concentrations are, from left to right, 50, 100, 25, and 75 percent. (B) NMR image of phantom immersed in H_2O showing variations of H_2O concentrations among the four chambers. (C) Single NMR line scan taken before immersion of phantom in H_2O. Peaks are labeled with H_2O concentrations as deduced from the NMR data. (D) Single NMR line scan of phantom immersed in H_2O. The two extra side peaks arise from the water simulating the chest wall.

0036-8075/82/0618-1313$01.00/0

Table 1. Comparison of water content of saline-filled and normal lung as obtained from wet and dry weight measurements and average NMR signals.

Preparation	Weight difference* (g of H_2O)	Dry weight (g)	Weight difference/ dry weight	Average NMR signal	(A)/(B)†	(C)/(D)‡
Isolated lung						
Right lung (with saline)	0.467	0.099	4.72 (A)	30.0 (C)	1.67	1.82
Left lung	0.167	0.059	2.83 (B)	16.5 (D)		
In situ lung						
Right lung, lower lobe (with saline)	0.759	0.085	8.93 (A)	17.0 (C)	2.64	2.50
Left lung and rest of right lung	0.612	0.181	3.38 (B)	6.80 (D)		

*Wet weight minus dry weight. †Ratio of gravimetric water contents of saline-filled and normal lung. ‡Ratio of NMR signal intensities of saline-filled and normal lung.

application of three perpendicular field gradients and two RF pulses. The specimen and field gradients are arranged in such a way that the line of excited nuclei is centered in the most homogeneous portion of the magnetic field. The specimen's position is then shifted slightly and the process repeated to excite a neighboring line of atoms. In this way an image of an entire slice can be produced in which all the nuclei are in the homogeneous portion of the field when they are being imaged.

The time required to collect data from the atoms in a single line was 25 msec without signal averaging. With signal averaging, it is important to wait at least T_1 (~ 0.3 second) between pulse sequences so that effects due to T_1 are minimized. For all the images reported here, 8 seconds were required for 16 averages on each line.

We constructed a phantom containing four disk-shaped chambers filled with $CuSO_4$-doped solutions of H_2O and D_2O, with initial H_2O concentrations of 50, 100, 25, and 75 percent (Fig. 1A). (In our experiments, the protons of H_2O and HDO are not distinguishable.) This is a convenient way to simulate various concentrations of H_2O, since D_2O will not produce an NMR signal at the proton frequency. Each chamber was 1/8 inch thick and was separated from the neighboring chambers by 1/8-inch-thick walls of Plexiglas. The phantom was immersed in a plastic vial filled with 100 percent H_2O to simulate a chest wall.

Conventional nonimaging NMR was used to determine the decreasing water content of an isolated fragment of rat lung as it dried (Fig. 2A). For the NMR lung imaging studies, we used only dead animals or isolated lungs in order to eliminate effects of heart and lung motion, even though we have obtained satisfactory NMR images of the heart and lungs of a living, spontaneously breathing rat. Sprague-Dawley rats were anesthetized with thiamylal sodium and the lungs removed after cannulation of the trachea. The lungs, enclosed in a plastic container to minimize evaporative water loss, were placed in the magnetic field with the long axis oriented vertically. The degree of inflation of the lungs was controlled by an adjustable constant-pressure source. Localized lung edema was simulated by (i) instilling normal saline into the right lung of an isolated preparation consisting of the right and left lungs and (ii) instilling normal saline into the right lower lobe of an intact dead rat (killed with 18 mg of Nembutal injected intraperitoneally). In the latter experiment, a Silastic tube (just fitting into the trachea) was advanced into the right lower lobe bronchus while both lungs were maintained at constant volume. One milliliter of air was then removed from the right lower lobe and replaced by 1 ml of normal saline. (A postmortem examination revealed the Silastic tube in the right lower lobe bronchus and confirmed the presence of isolated right lower lobe edema.) We determined lung water content by NMR and calculated, after gravimetric measurement (*8*), the water content per unit of dry lung weight [(wet weight − dry weight)/dry weight].

A photograph of the phantom in air is shown in Fig. 1A. The NMR image of the H_2O in a 2-mm slice through the median plane of the phantom immersed in H_2O is shown in Fig. 1B. The brightest regions in Fig. 1B contain the largest H_2O concentrations. Plots of single line scans from the phantom in air (Fig. 1C) and in H_2O (Fig. 1D) provide quantitative determinations of H_2O concentrations. The detected peak values (normalized to the 100 percent H_2O peak in Fig. 1, C and D) lie within a few percent of the predetermined values (left to right; 50, 100, 25,

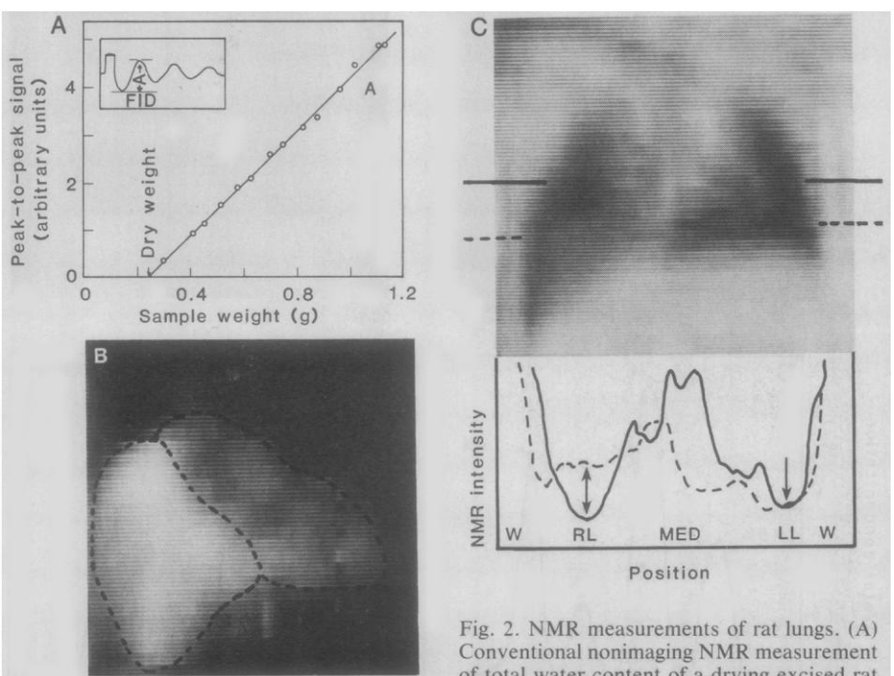

Fig. 2. NMR measurements of rat lungs. (A) Conventional nonimaging NMR measurement of total water content of a drying excised rat lung fragment. (B) NMR image of a pair of isolated rat lungs after normal saline instillation in the right lung (on left in photograph). The sketch shows the outline of each lung. (C) NMR image and line-scan plots of lung water content of an intact dead rat after right lower lobe (RLL) intrabronchial normal saline instillation. The solid and dashed lines in the image correspond to those in the graph and indicate the line scan through normal lung and through the saline-filled RLL, respectively. Abbreviations: *W*, chest wall; *RL*, right lung signal; *MED*, mediastinum; *LL*, left lung signal. Single-head arrow indicates lack of difference between solid and dashed lines; double-head arrow indicates difference between solid (no saline) and dashed (saline in RLL) lines.

and 75 percent H_2O) and were not influenced significantly by immersion of the phantom in the H_2O simulating the chest wall. For the three peaks in Fig. 1, C and D, from H_2O/D_2O mixtures of 50, 25, and 75 percent H_2O, the average absolute deviation from the predetermined H_2O concentrations was 2.7 percent. When one of the tubes in Fig. 1A was filled with whole human blood, the NMR signal intensity was 82 percent of the signal from pure H_2O, indicating that 82 percent of the blood was H_2O. This result compares well with published confidence limits for H_2O in whole human blood of 83 to 86.5 percent (*9*).

Conventional NMR measurement of the total water content of an excised drying lung fragment was validated by weighing the fragment after each NMR measurement of the free induction decay (FID) following an excitation pulse (Fig. 2A). The extrapolated sample weight at zero NMR signal (dry weight) was determined from a least-squares regression to be 0.234 g, which was 98 percent of the gravimetric dry weight (0.248 g).

Regional lung edema, simulated by saline instillation, was detected by NMR in both the right lung of an isolated lung preparation (Fig. 2B) and the right lower lobe of an in situ lung (Fig. 2C). Good agreement was observed between the ratio of gravimetric water contents [(*A*)/(*B*)] and the ratio of NMR signal intensities [(*C*)/(*D*)] of the normal and saline-filled lungs (both the isolated right lung and the in situ right lower lobe) (Table 1).

These results provide evidence of the power of NMR imaging as a technique for performing quantitative studies of lung water. It is a noninvasive, perfusion- and ventilation-independent, technique that shows promise of becoming the standard method for in vivo measurement of the absolute amount of lung water and its distribution.

CECIL E. HAYES
THOMAS A. CASE
DAVID C. AILION
Department of Physics, University of Utah, Salt Lake City 84112
ALAN H. MORRIS
Pulmonary Divisions, Departments of Medicine, University of Utah, and *LDS Hospital, Salt Lake City 84143*
ANTONIO CUTILLO
Pulmonary Division, Department of Medicine, University of Utah
CELIA W. BLACKBURN
CARL H. DURNEY
Department of Electrical Engineering, University of Utah
STEVEN A. JOHNSON
Department of Bioengineering, University of Utah

References and Notes

1. I. L. Pykett and P. Mansfield, *Phys. Med. Biol.* **23**, 961 (1978).
2. W. A. Edelstein, J. M. S. Hutchison, G. Johnson, T. Redpath, *ibid.* **25**, 751 (1980).
3. P. C. Lauterbur, paper presented at the Engineering Foundation Conference on Comparative Productivity of Techniques for Noninvasive Medical Diagnosis, Henniker, N.H., August 1976.
4. J. A. Frank, thesis, State University of New York, Stony Brook (1977).
5. R. Casaburi, K. Wasserman, R. M. Effros, in *Lung Water and Solute Exchange*, N. C. Staub, Ed. (Dekker, New York, 1978), pp. 323–375.
6. C. P. Slichter, *Principles of Magnetic Resonance* (Springer-Verlag, Berlin, ed. 2, 1980).
7. L. E. Crooks, *IEEE Trans. Nucl. Sci.* **NS-27**, 1239 (1980).
8. A. C. Guyton and A. W. Lindsey, *Circ. Res.* **7**, 649 (1959).
9. F. E. Davis, K. Kenyon, J. Kirk, *Science* **118**, 276 (1953).

10. Supported by grant 2 R01 HL 23746-03 from the National Institutes of Health.

22 September 1981; revised 26 January 1982

Deep-Sea Bacteria: Isolation in the Absence of Decompression

Abstract. *Sampling and pure culture isolation of deep-sea bacteria without loss of in situ pressure is required in order to determine the viability of decompression-sensitive strains. This was achieved by using a pressure-retaining sterilizable seawater sampling system in connection with a prepressurized hyperbaric isolation chamber. Rates of growth and substrate uptake of the majority of isolates showed highly barotolerant characteristics, while the remainder (4 out of 15) exhibited barophilic characteristics.*

During the last decade, deep-sea microbiology advanced in three areas, namely, the development of pressure-retaining sampling equipment (*1*, *2*), in situ studies with the research submersible *Alvin* (*3*), and the isolation of specifically pressure-adapted, barophilic bacteria (*4*). This work has led to a general understanding of the fact that the microbial decomposition and remineralization of natural and man-made materials on 60 percent of the globe's surface, covered by seawater of a depth of 1000 m or more, are strongly influenced by conditions characteristic of the deep sea. These are primarily the generally low concentrations of metabolizable organic substrates, uniformly low temperatures of 2° to 3°C, and hydrostatic pressure which increases approximately 1 atm for every 10 m of depth (*5*).

Microbial adaptations to life at extremely low nutrient levels (*6*) and low temperatures (*7*) have been well studied. Cold-adapted, psychrophilic bacteria, growing optimally at about 8° to 15°C, do not survive temperatures in the range of 20° to 25°C. In response to pressure,

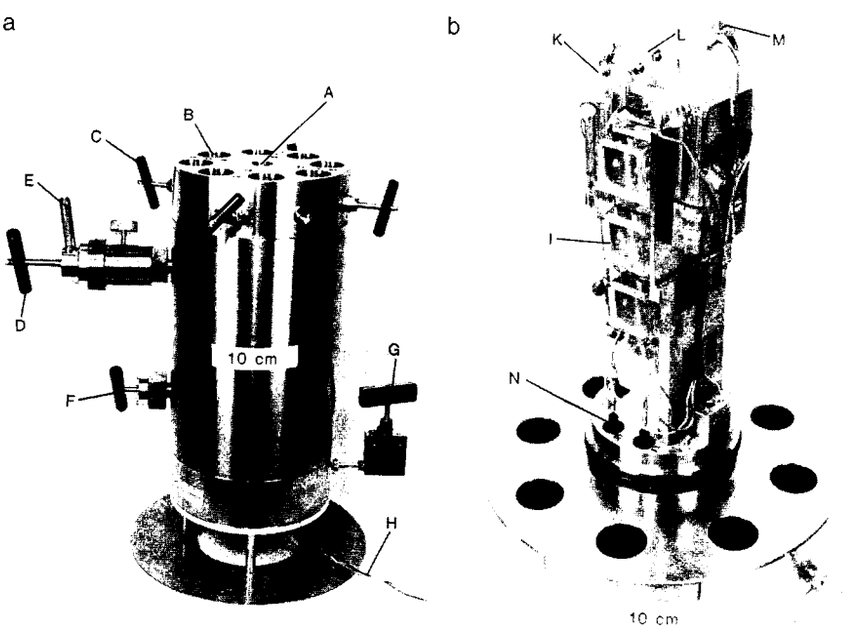

Fig. 1. (a) Isolation chamber assembled. *A*, viewing window; *B*, reset end cap bolts; *C*, valves for sample transfer into four vials; *D*, handle for horizontal movement of streaking loop; *E*, lever for rotary movement of streaking loop; *F*, handle for movement of agar plates; *G*, valve for pressurization; and *H*, wires for illumination and loop sterilization. (b) Bottom end cap with inner parts of isolation chamber (top removed); *I*, agar plates (nine); *K*, vials for liquid medium (four); *L*, ceramic loop holder with streaking loop; *M*, halogen lamps (five); and *N*, wire penetrators.

0036-8075/82/0618-1315$01.00/0